# Correspondence

## A High Average Power Broad-Band Ferrite Load Isolator for *S* Band*

A broad-band high average power *S*-band load isolator has been developed by using a dielectric loaded waveguide and a composite ferrite. A partial height dielectric was centrally mounted on the broadwall of a vertically constricted *S*-band waveguide, Fig. 1. The cross section dimensions of the dielectric were chosen to increase the operating bandwidth of the isolator. Adjacent to either side of the dielectric 2 thin flat slabs of ferrite were positioned. A large ratio of ferrite width to thickness was chosen to achieve maximum heat dissipation. The ferrite element was composed of 2 ferrite types. Towards the source end of the isolator a long length of a narrow resonance linewidth and low dielectric loss ferrite was mounted. This portion of the ferrite element provided the majority of the isolation loss. However, since this ferrite possessed only a moderate Curie temperature the average effective power handling capacity of the isolator composed of this ferrite alone was limited to less than 1600 watts. To maintain a large value of the isolation loss in the presence of an appreciable load mismatch a second ferrite piece of a higher Curie temperature ferrite was employed. A small length of the higher Curie temperature ferrite was mounted adjacent to the first ferrite and towards the load end of the isolator. The length of the second ferrite was chosen to provide 3 to 4 db isolation loss.

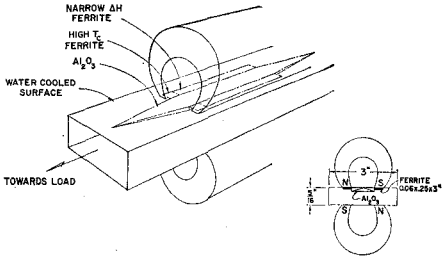


Fig. 1—Basic elements of the high-power *S*-band isolator.

A skew transverse magnetizing field was employed which assisted in increasing the bandwidth of the isolator. Magnetic field skewing was produced by magnetizing the upper and lower permanent magnets unequally. A reduction of magnet size was accomplished by employing a vertically constricted waveguide at some sacrifice of the peak power handling capacity.

High average power performance was measured with a nominal 600–800-watt CW magnetron tunable over the 2.5 to 3.7-kmc band. Isolation loss was checked at low and high powers. Measurements of insertion loss were made in detail at low power and checked at selected frequency points at high power. This simplification in measurement was permissible since it was found that insertion loss decreased very slightly at the higher average powers.

In addition to isolation and insertion loss the power absorbed by the ferrite was determined with the isolator operating at high average power in the reverse direction. This technique enables the simulation of high average power operation with moderate power sources. From a knowledge of these quantities it is possible to compute the effective average power capacity, $P_{eff}$, of the isolator when operating into a given load mismatch as follows:

$$P_{eff}(1 - T_F) + \Gamma T_F P_{eff}(1 - T_R) = P_{abs}$$

$$P_{eff} = \frac{P_{abs}}{1 + T_F\Gamma\left(1 - T_R - \frac{1}{\Gamma}\right)}$$

where $P_{abs}$ is the average power absorbed by the ferrite in the reverse direction.

$\Gamma$ is the power reflection coefficient of the load.

$T_F$ is the isolator power transmission coefficient in the insertion loss direction.

$T_R$ is the power transmission coefficient in the isolation loss direction.

The computed effective power capacity yields a value which is less than the actual power capacity. This discrepancy occurs because the present measurement of the absorbed power is made under conditions wherein the heat absorbed is concentrated in a limited portion of the ferrite length. In practice a large proportion of the dissipated power would be more uniformly distributed throughout the sample as a result of the insertion loss absorption.

For the ferrites and ferrite geometry employed in these studies, high-power nonlinear phenomena were not evident. In experimental circumstances, where ferrites of lower resonance line width or higher saturation magnetizations are employed, or where higher RF powers and ferrite geometries more susceptible to spin wave instabilities are utilized, direct measurement of isolator performance at the rated power levels must be made to evaluate the nonlinear effects.

Fig. 2 presents performance data taken for a water cooled isolator operating at 2 effective power levels; milliwatt and greater than 1650 watts CW (2:1 load mismatch). The ferrite element consisted of a combination of magnesium manganese and nickel ferrite slabs positioned as shown in Fig. 1. The isolation to insertion loss db ratio manifested while the unit was absorbing 400 watts CW in the reverse direction was found to be in excess of 20/1 over greater than 15 per cent bandwidth.

Fig. 3 presents performance data for an isolator constructed from a single type of

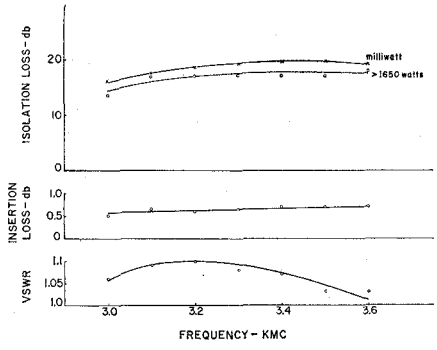


Fig. 2—Performance data for a high-power load isolator using magnesium manganese R-1 and nickel ferrite 106.

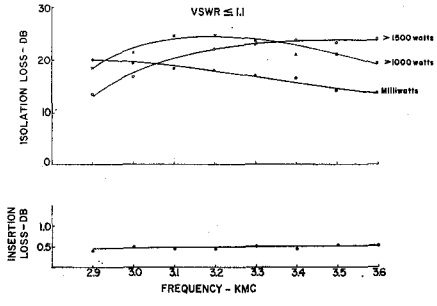


Fig. 3—Performance data for a high-power load isolator using $Ni_{0.7}Cu_{0.3}Mb_{0.02}Fe_{1.9}O_4$ ferrite.

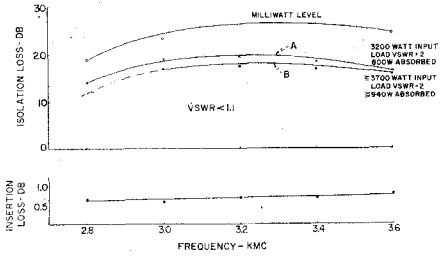


Fig. 4—Performance data for a high-power load isolator using $Ni_{0.7}Cu_{0.3}Mn_{0.02}Fe_{1.9}O_4$ and nickel ferrite, ferroxcube 106.

nickel ferrite of composition $Ni_{0.7}Cu_{0.3}Mn_{0.02}Fe_{1.9}O_4$. A noticeable frequency shift of the peak isolation occurs as the power is raised. The shift of the resonance peak toward the higher frequencies arises from the decrease of saturation magnetization of the ferrite that accompanies ferrite heating.

Fig. 4 shows performance data of an isolator constructed with the nickel ferrite used in Fig. 3 plus a portion of a higher Curie temperature nickel ferrite. Ferroxcube 106, positioned on the load end of the unit. The effective power capacity when operating into a 2/1 load mismatch exceeded 3000 watts CW for 14 db or greater isolation and 0.6 db or less insertion loss throughout the 2.8 to greater than 3.6 kmc band (>25 per cent bandwidth). A greater than 3700-watt effective average power capacity is shown

* Received by the PGMTT, August 4, 1958.

for curve $B$. A comparison of the data of Figs. 3 and 4 reveals the improvement in average power handling capacity obtained by using a high Curie temperature tip of ferrite positioned on the load end. The trend of decreasing isolation loss at the low end of the band as the effective power is raised is markedly reduced in Fig. 4, where, for the composite ferrite isolator, isolation loss at 2.9 kmc is greater than 15 db for an effective average input power of 3200 watts. Without the high Curie temperature ferrite the isolator of Fig. 3 displays a reverse loss of <13 db at 2.9 kmc for an effective average input of only 1500 watts.

E. N. Skomal
Sylvania Microwave Phys. Lab.
Mountain View, Calif.

## Reflection Coefficient of $E$-Plane Tapered Waveguides*

In a paper by Matsumaru,[1] formulas of the input reflection coefficients of the linearly and sinusoidally $E$-plane tapered waveguides are given. Excellent agreements between the theoretical and experimental results have been found in both cases. In this note we wish to add some analytical remarks.

The analysis given in the above paper is different from the rigorous one given by Walker and Wax.[2] The latter led to a nonlinear differential equation

$$\frac{dR}{dx} - 2\gamma R + \frac{1-R^2}{2}\frac{d}{dx}\ln[Z(x)] = 0 \quad (1)$$

where $R$ is the reflection coefficient, $Z(x)$ is the surge impedance of the tapered line, and $\gamma=\alpha+j\beta$ is the wave propagation constant. If the tapered line is loss-free, then we have $\gamma=j\beta$. On the assumption that the phase constant, $\beta$ is independent of $x$, and that $R^2\ll 1$, Bolinder[3] obtained an approximate expression of the input reflection coefficient

$$R = \frac{1}{2}\int_0^l \frac{d}{dx}[\ln Z(x)]\cdot e^{-j2\beta x}dx \quad (2)$$

for a finite tapered line of length $l$, terminated by $Z(0)=Z_1$ and $Z(l)=Z_2$ at each end.

It may be shown that Mr. Matsumaru's equations (4) and (12) are equivalent to (2) in this communication. On substitution of the surge impedance of a sinusoidal taper

$$Z(x) = \frac{Z_1+Z_2}{2} - \frac{Z_1-Z_2}{2}\cos\left(\frac{\pi x}{l}\right) \quad (3)$$

into our (2), we obtain his (12). Substituting the surge impedance of a linear taper

$$Z(x) = Z_1 + (Z_2 - Z_1)x/l \quad (4)$$

into our (2), and letting $x=y+l/2$, we obtain his (4), with its independent variable $x$ being replaced by $y$. Therefore, it appears that Bolinder's assumption of $R^2\ll 1$ should also apply to Mr. Matsumaru's analytical results. This is not, however, stated explicitly in his paper.

For a linearly tapered line defined by (4), (2) may be integrated exactly in terms of $Ci$ and $Si$, the cosine and sine integrals. The input reflection coefficient is

$$R = \tfrac{1}{2}e^{ju_2}\{[Ci(u_2) - Ci(u_1)] - j[Si(u_2) - Si(u_1)]\} \quad (5)$$

where $u_1=2\beta l/(k-1)$, $u_2=2\beta lk/(k-1)$ and $k=Z_2/Z_1$. This expression appears to be somewhat simpler than Mr. Matsumaru's (8), and his (7), a binomial-expansion approximation, is not necessary in this case. If a change of variable, $u=2\beta(q^{-1}+x)$, is made, his (5) leads directly to the above result—our (5).

In the treatment of a sinusoidally tapered line, noting that $r=(Z_1-Z_2)/(Z_2+Z_1)$ tends to zero first, and letting $l$ tend to zero next, Mr. Matsumara showed how his (15) becomes

$$R = (Z_2 - Z_1)/(Z_2 + Z_1),$$

the reflection coefficient of two directly connected waveguides. It is felt that this statement, although correct, might mislead one to think that Matsumaru's (12) is exact. To clarify this point, we let $l$ in his (15) tend to zero first and retain the higher order terms; (15) then becomes

$$\lim_{l\to 0} R = \left(\frac{Z_2-Z_1}{Z_2+Z_1}\right) + \frac{1}{3}\left(\frac{Z_2-Z_1}{Z_2+Z_1}\right)^3 + \cdots = \frac{1}{2}\ln\frac{Z_2}{Z_1}.$$

It is seen that as $l$ tends to zero, $R$ tends to $\frac{1}{2}\ln(Z_2/Z_1)$ rather than to $(Z_2-Z_1)/(Z_2+Z_1)$. This limiting case indicates somewhat the approximate nature of Matsumaru's (12), from which his (15) is derived. It might be said that the approximation becomes increasingly good as $r$ tends to zero; then

$$\lim_{l\to 0} R = \frac{1}{2}\ln\frac{Z_2}{Z_1} \cong \frac{Z_2-Z_1}{Z_2+Z_1}.$$

It is also noted that our (5) also becomes $\frac{1}{2}\ln(Z_2/Z_1)$ as $l$ tends to zero. As long as we use our (2) or its equivalent—Mr. Matsumaru's equations (4) and (12)—this is true, regardless of the nature of $Z(x)$ or type of taper. This can be seen directly from our (2), in which the phase factor tends to unity as $l$ tends to zero. Direct integration gives the proof.

Eq. (2) in this demonstration may be considered as the first approximation of the solution to our differential equation (1), which—together with higher order approximations—has been discussed elsewhere.[4] In general it may be said that if the length of taper is longer than half of a guide-wavelength, the second order approximation has no significant effect.

Richard F. H. Yang
Andrew Corporation
Chicago, Illinois

### *Author's Comment*[5]

I am grateful to Mr. Yang for his remarks regarding my paper; his detailed remarks strengthen some of the weak points in it.

First, his analysis of his (4) is known to me, and I have no further comments to make on it. Next, his formula (5) is probably quite useful in calculating the reflection coefficient of linear tapers. In the latter part of his communication, he has made some remarks on the limiting cases of $R$. Although I had previously considered these analytical studies, I did not discuss them fully since they seemed to be too detailed for my paper.

As I mentioned in my paper, the main purpose was to present practical design data rather than detailed analyses. I would like to take this opportunity to add some comments on the experimental data described in my paper. Figs. 1 and 2, plotted in the $K$-plane,

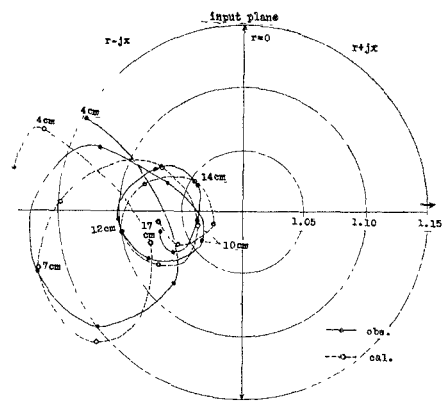


Fig. 1—Results of experiments, part I ($Z_2/Z_1=2.0$). Data are shown for linear-taper lengths from 4 to 17 cm.

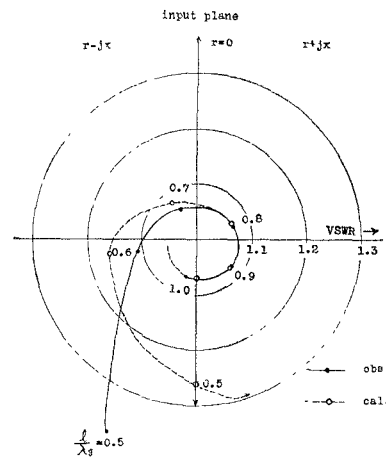


Fig. 2—Results of experiments, part III ($Z_1/Z_2=2.4$). The normalized sinusoidal-taper length $l/\lambda_g$ was varied from 0.5 to 1.0.

show the reflection coefficients of the data obtained from experiments, parts I and III, respectively. The conically looped circular loci of $R$ of the linear tapers in Fig. 1 show the typical behavior for the cases of $Z_2>Z_1$. It should be mentioned that the position of $R$ follows almost the course of one conical cycle every half-wavelength (4.9 cm). For

Received by the PGMTT, August 4, 1958

* Received by the PGMTT, June 30, 1958.

[1] K. Matsumaru, "Reflection coefficient of $E$-plane tapered waveguides," IRE Trans. on Microwave Theory and Techniques, vol. MTT-6, pp. 143–149, April, 1958.

[2] L. R. Walker and N. Wax, "Non-uniform transmission lines and reflection coefficients," *J. Appl. Phys.*, vol. 17, pp. 1043–1045; December, 1946.

[3] F. Bolinder, "Fourier transforms in the theory of inhomogeneous transmission lines," Proc. IRE, vol. 38, p. 1354; November, 1950.

[4] L. Solymar, "On higher order approximations to the solution of nonuniform transmission lines," Proc. IRE, vol. 45, pp. 1547–1548; November, 1957.